

Disorder-dependent superconducting pairing symmetry in doped graphene

Kaiyi Guo*,¹ Yue Zhang,^{1,*} Ying Liang,^{1,2} and Tianxing Ma^{1,2,†}

¹*School of Physics and Astronomy, Beijing Normal University, Beijing 100875, China*

²*Key Laboratory of Multiscale Spin Physics(Ministry of Education),
Beijing Normal University, Beijing 100875, China*

Disorder and doping have profound effects on the intrinsic physical mechanisms of superconductivity. In this paper, we employed the determinant quantum Monte Carlo method to investigate the symmetry-allowed superconducting orders on the two-dimensional honeycomb lattice within the Hubbard model, using doped graphene as the carrier, focusing their response to bond disorder. Specifically, we calculated the pairing susceptibility and effective pairing interactions for the $d + id$ wave and extended s -wave pairings for different electron densities and disorder strengths. Our calculations show that at high electron densities, increased disorder strength may lead to a transform from $d + id$ wave dominance to extended s wave dominance. However, at lower electron densities, neither of the two superconducting pairings appears under larger disorder strength. Our calculations may contribute to a further understanding of the superconducting behavior in doped materials affected by disorder.

I. INTRODUCTION

Unconventional superconductivity is one of the most important subjects in modern condensed matter physics, and in past decades, the fabrication of superconducting materials and understanding on the pairing mechanism have attracted the attention of numerous researchers [1, 2]. Inevitably, the experimental preparation of superconducting materials with doping electrons or holes shall introduce disorder into the system, and the presence of disorder will alter the material's properties [3]. For example, researchers have found that disorder may raise [4, 5] or decrease [6, 7] the superconducting transition temperature, or may have no effect on it [7, 8]. In comparison to clean systems, stronger disorder increases spatial inhomogeneity, thereby enhancing localization and the superconducting energy gap [9]. Through numerical computations, the researchers have found that disorder leads to the formation of islands with higher superconducting order, consequently causing the system to undergo a superconducting-insulator transition [10–13]. However, it is worth noting that correlated disorder may have a contrasting influence on the system, rendering superconductivity more robust [14]. Related experimental results also respond to the complicated response of superconductivity to disorder [15–17].

Behind all of the above marvelous phenomena, the role played by disorder remains a question of great interest. To investigate the influence of disorder on superconductivity, an essential idea is to explore its effect on the superconducting pairing symmetry. As one of the key superconducting order parameters, the pairing symmetry plays an important role in the study of superconductivity, determining the physical properties of the superconducting state [18, 19], which attract

the attention of both experimental and theoretical researchers [20–22]. After extensive research since the discovery of doped cuprates, the pairing mechanism of superconductivity continues to remain enigmatic. It has become relatively clear that d -wave pairing dominates in doped cuprates [23–25], while iron-based superconductors are primarily driven by s_{\pm} wave pairing [26, 27]. The situation becomes more intricate in the case of nickel-based superconductors, in which both d -wave and s -wave superconducting gaps are observed [28–30].

Recently, superconductivity in graphene-based systems has attracted a lot of attention [31–49]. Researchers have shown evidence for triggered superconducting density of states by placing monolayer graphene on d -wave superconductors [32]. Subsequently, studies have also demonstrated gate-tunable high-temperature superconducting proximity effects in monolayer graphene [33]. Since march of 2018, the observation of superconducting phenomena on magic-angle graphene superlattices generated great excitement [34, 35]. Among them, different pairing symmetry, for example, $d + id$ [36–38], $p + ip$ [39, 40], as well as extensive s (ES) [41] waves are proposed in different situations or within different models. Thus, the doped graphene-based materials provide an interesting platform for investigating superconducting pairing symmetries, which may lead further understanding on the pairing mechanism [38, 42–44].

Naturally, doping and disorder are both present in real materials [50, 51]. In this paper we investigated the dominant superconducting pairing symmetry in doped graphene with bond disorder. The disorder induced a finite density of state in lightly doped graphene, which is different from clean system. It is found that the introduced disorder not only increase the effective pairing interaction, but also lead to a transform in the dominant pairing symmetry. Our primary findings are presented in the form of a superconducting pairing in Fig.1, which shows that the symmetry of pairing is not only related to the strength of disorder, but also to the electron density.

* These authors contributed equally to this work.

† txma@bnu.edu.cn

When the strength of disorder is small, pairing with $d + id$ symmetry dominates with ES symmetry, which is consistent with previous results [47]. However, the situation is different when the disorder strength is large. Near half-filling where the electron density is large, with the increasing of the disorder strength, the $d + id$ wave is suppressed, while the ES wave is strengthened, and when the disorder strength exceeds a critical value, the system's superconducting pairing shall be dominated by the ES wave. Through the analysis of the effective pairing interaction $P_\alpha - \tilde{P}_\alpha$, we find that in instances of large disorder strength and low electron density, both value of $P_{d+id} - \tilde{P}_{d+id}$ and $P_{ES} - \tilde{P}_{ES}$ are negative and there is no longer an effective attractive interactions between the electrons. Consequently, neither $d + id$ wave nor the ES wave exists. The actual situation in this case may be even more intricate. More detailed computational results will be discussed in the following sections.

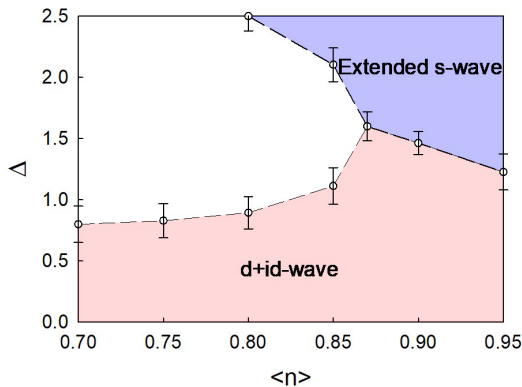


FIG. 1. Illustration of superconduction pairing of doping-dependent disordered Hubbard model on honeycomb lattice, considering the lattice size of $N_s = 96$, and the temperature of $\beta = 10$. Δ labels the disorder strength and $\langle n \rangle$ represents the electron density.

II. MODEL AND METHODS

The low-energy electronic and superconducting property of graphene can be well described by the disordered Hubbard model on a honeycomb lattice [52]:

$$\hat{H} = - \sum_{\langle \mathbf{i}, \mathbf{j} \rangle, \sigma} t_{\mathbf{ij}} (\hat{c}_{\mathbf{i}\sigma}^\dagger \hat{c}_{\mathbf{j}\sigma} + \hat{c}_{\mathbf{j}\sigma}^\dagger \hat{c}_{\mathbf{i}\sigma}) - \mu \sum_{\mathbf{i}\sigma} \hat{n}_{\mathbf{i}\sigma} + U \sum_{\mathbf{i}} \hat{n}_{\mathbf{i}\uparrow} \hat{n}_{\mathbf{i}\downarrow} \quad (1)$$

Here, $\hat{c}_{\mathbf{i}\sigma}^\dagger$ ($\hat{c}_{\mathbf{j}\sigma}$) is the creation (annihilation) operator of an electron with spin σ at site \mathbf{i} (\mathbf{j}), and $\hat{n}_{\mathbf{i}\sigma} = \hat{c}_{\mathbf{i}\sigma}^\dagger \hat{c}_{\mathbf{i}\sigma}$ is the number operator, denoting the number of spin- σ electrons at site \mathbf{i} . μ is the chemical potential which

determines the density of the system, when $\mu = \frac{U}{2}$, $\langle n \rangle = 1$, the system is half-filled, indicating the particle-hole symmetry. When deviating from half-filling, the corresponding μ for a specific $\langle n \rangle$ varies with a different set of parameters. Therefore, for each set of parameters, we have individually tuned the chemical potential μ to fix the specific electronic density $\langle n \rangle$. $t_{\mathbf{ij}}$ represent the hopping amplitude between two nearest-neighbor sites \mathbf{i} and \mathbf{j} , and the bond disorder is induced by modifying the matrix element $t_{\mathbf{ij}}$ of the hopping matrix, which is chosen from $t_{\mathbf{ij}} \in [t - \Delta/2, t + \Delta/2]$ and zero otherwise with a probability $P(t_{\mathbf{ij}}) = 1/\Delta$. The strength of disorder can be characterized by Δ , which represents the magnitude of the modification of matrix elements $t_{\mathbf{ij}}$. The parameter t is set as $t = 1$ as the energy scale. Here $U > 0$ represents the on-site repulsive interaction. In this article, we mainly use $U = 3|t|$. In the presence of disorder, reliable results are obtained by taking an average of 20 disorder simulations, as it has been demonstrated to effectively avoid errors introduced by randomness [53, 54].

Our simulations are mostly performed on lattices of double-48 sites with periodic boundary conditions. The double-48 lattice implies a total number of sites $N_s = 2 \times 3 \times 4^2 = 96$ [47]. The finite-temperature determinant quantum Monte Carlo (DQMC) method is employed to complete simulations. The basic strategy of the DQMC is to express the partition function $Z = \text{Tr} e^{-\beta H}$ as a path integral over a set of random auxiliary fields. The imaginary time interval $(0, \beta)$ is discretely divided into M slices of interval $\Delta\tau$, which is chosen as small as 0.1 to control the ‘‘Trotter errors.’’

To investigate the superconducting property of graphene, the pairing susceptibility is computed:

$$P_\alpha = \frac{1}{N_s} \sum_{i,j} \int_0^\beta d\tau \langle \Delta_\alpha^\dagger(i, \tau) \Delta_\alpha(j, 0) \rangle, \quad (2)$$

where α stands for the pairing symmetry. Due to the constraint of the on-site Hubbard interaction in Eq.(1), pairing between two sublattices is favored and the corresponding order parameter $\Delta_\alpha^\dagger(i)$ is defined as

$$\Delta_\alpha^\dagger(i) = \sum_l f_\alpha^\dagger(\delta_l) (c_{i\uparrow} c_{i+\delta_l\downarrow} - c_{i\downarrow} c_{i+\delta_l\uparrow})^\dagger \quad (3)$$

with $f_\alpha(\delta_l)$ being the form factor of pairing function. The vector δ_l ($l = 1, 2, 3$) denotes the nearest-neighbor (NN) connection. Considering the honeycomb lattice symmetry of the D6 point group, two possible NN pairing symmetries are characterized: (i) ES wave, and (ii) $d + id$ wave.

$$ES \text{ wave} : f_{ES}(\delta_l) = 1, \quad l = 1, 2, 3 \quad (4)$$

$$d + id \text{ wave} : f_{d+id}(\delta_l) = e^{i(l-1)\frac{2\pi}{3}}, \quad l = 1, 2, 3 \quad (5)$$

III. RESULTS AND DISCUSSION

We first investigated the variation of the pairing susceptibility P_{ES} and P_{d+id} with temperature for the electron density close to half filling, $\langle n \rangle = 0.95$, as shown in Fig.2. The solid lines represent the $d + id$ pairing symmetries while the dashed lines represent the ES pairing symmetries. By choosing the disorder strengths $\Delta = 0.0, 1.5$, and 2.5 , it can be observed that P_α always increases with decreasing temperature, and the bond disorder suppresses P_α . In the clean limit, i.e., $\Delta = 0.0$, P_{d+id} increases faster than P_{ES} at low temperatures, indicating the dominance of the $d + id$ wave over the ES wave. At $\Delta = 1.5$, the values of the two symmetries are almost equal within the range of our calculations. With a larger disorder strength, at $\Delta = 2.5$, P_{ES} increases faster than P_{d+id} at low temperatures, indicating that the ES wave dominates over the $d + id$ wave at this time. By varying the strength of the bond disorder, we find that the magnitude of Δ alters the superconducting pairing symmetry dominating.

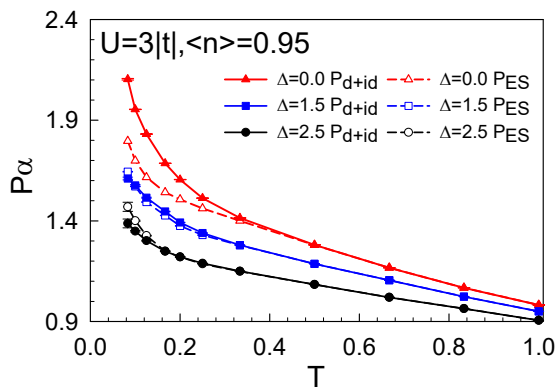


FIG. 2. Pairing susceptibility P_α as a function of temperature T for different pairing symmetries P_{ES} , P_{d+id} , and different disorder strength Δ with electron density $\langle n \rangle = 0.95$.

In order to make a further investigation into the superconducting pairing symmetry, we shall replace $\langle c_{i\uparrow}^\dagger c_{j\uparrow} c_{i+\downarrow}^\dagger c_{j+\downarrow} \rangle$ with $\langle c_{i\uparrow}^\dagger c_{j\uparrow} \rangle \langle c_{i+\downarrow}^\dagger c_{j+\downarrow} \rangle$ in Eq.(2) to obtain the bubble contribution \tilde{P}_α , thereby extracting the effective pairing interactions in different pairing channels. In Fig. 3, we compare the variations of P_α and \tilde{P}_α with temperature for different disorder strengths Δ and pairing symmetries. Figure 3(a) represents the $d + id$ wave, while Fig. 3(b) represents the ES wave. It can be clearly seen that with the increase in Δ , both P_α and \tilde{P}_α are suppressed, and P_α is always larger than \tilde{P}_α , which signifies that the effective pairing interactions persistently maintain positive values. To visually emphasize the influence of parameters on the effective pairing interactions, we compute $P_\alpha - \tilde{P}_\alpha$, and the relevant results are shown in Fig. 4.

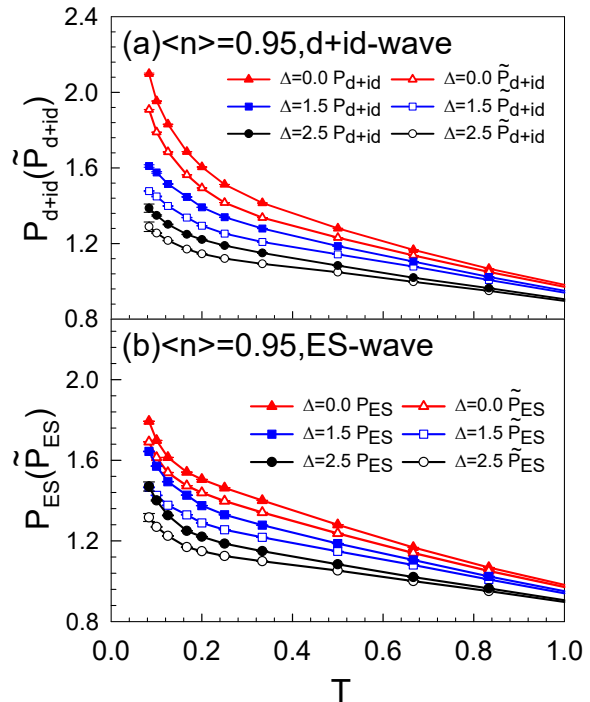


FIG. 3. Pairing susceptibility P_α and \tilde{P}_α as a function of temperature T for different disorder strength with electron density $\langle n \rangle = 0.95$. (a) $d + id$ wave and (b) ES wave

Figure 4 shows the temperature-dependent evolution of the effective pairing correlation $P_\alpha - \tilde{P}_\alpha$ in different pairing channels. It is evident that the effective pairing correlation is positive and tends to diverge at low temperatures in all cases, which indicates the presence of the attraction between electrons for both ES and $d + id$ pairing symmetries. Figure 4(a) illustrates the $d + id$ pairing symmetry. It is noteworthy that at $\langle n \rangle = 0.95$, the effective pairing correlation $P_{d+id} - \tilde{P}_{d+id}$ is suppressed with increasing disorder strength at low temperatures. Conversely, the effective pairing correlation $P_{ES} - \tilde{P}_{ES}$ increases with the increasing of disorder strength at low temperatures. These results can explain the shift in dominant superconducting pairing symmetry observed in Fig.2: the introduction of disorder will suppress $P_{d+id} - \tilde{P}_{d+id}$ while promoting $P_{ES} - \tilde{P}_{ES}$. This implies that bond disorder may lead to a variation in the dominant pairing symmetry in graphene from $d + id$ dominant to ES dominant. To illustrate the transform of the dominant pairing symmetry more clearly, we plot the effective pairing interaction as a function of Δ in Figs.4(c) and Fig.4(d) for fixed temperatures of $\beta = 10$ and $\beta = 12$, respectively. The results show that with increasing Δ , the dominant pairing symmetry transforms from the $d + id$ to the ES .

Having investigated the situation near half-filling, we now turn our attention to regions with higher

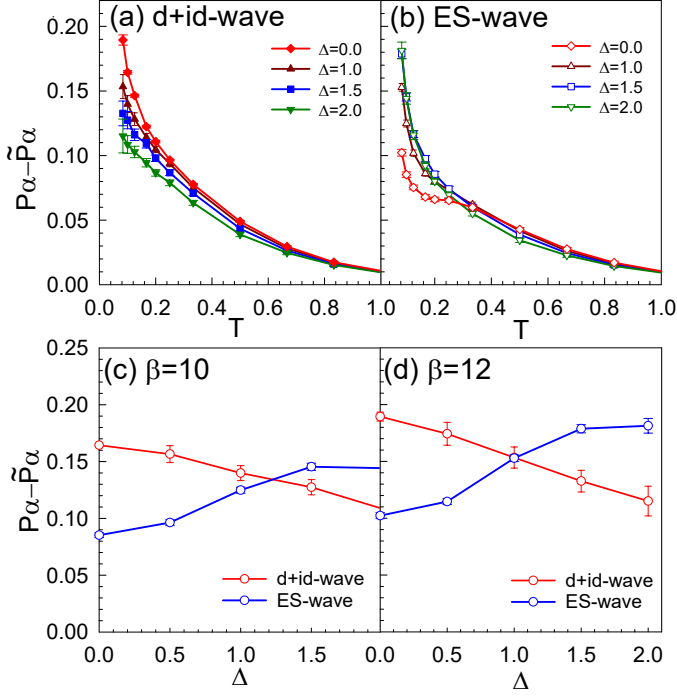


FIG. 4. The effective pairing interaction $P_\alpha - \tilde{P}_\alpha$ in different pairing channels (a) $d+id$ wave and (b) ES wave as a function of temperature T for different disorder strength with electron density $\langle n \rangle = 0.95$. (c) and (d) display the effective pairing interaction as a function of Δ , at the fixed temperatures of (c) $\beta = 10$ and (d) $\beta = 12$.

doping to see if the situation will be different. Figure 5 shows the temperature-dependent evolution of the pairing susceptibility P_{ES} and P_{d+id} at different disorder strengths for electron densities (a) $\langle n \rangle = 0.85$ and (b) $\langle n \rangle = 0.70$. Similar to the previous results, the solid lines represent the $d+id$ pairing symmetry and the dashed lines represent the ES pairing symmetry. It can be seen that, as before, disorder shows a suppressive influence on the pairing susceptibility for both $d+id$ and ES symmetries. Furthermore, with increasing disorder strength, the superconducting pairing transforms from $d+id$ wave dominance to ES wave dominance. Additionally, at lower electron densities and higher disorder strength, as the temperature decreases, P_{d+id} no longer diverges. This suggests the potential absence of $d+id$ wave. For a more in-depth analysis of the results, we present the temperature-dependent evolution of the effective pairing correlation $P_\alpha - \tilde{P}_\alpha$ in different channels for $\langle n \rangle = 0.85$ and $\langle n \rangle = 0.70$ in Figs. 6 and 7, respectively.

Figure 6 shows the temperature-dependent evolution of the effective pairing correlations (a) $P_{d+id} - \tilde{P}_{d+id}$ and (b) $P_{ES} - \tilde{P}_{ES}$ at $\langle n \rangle = 0.85$. It can be found that, in the clean limit, the system exhibits positive $P_{d+id} - \tilde{P}_{d+id}$, while negative $P_{ES} - \tilde{P}_{ES}$ is present. The introducing of

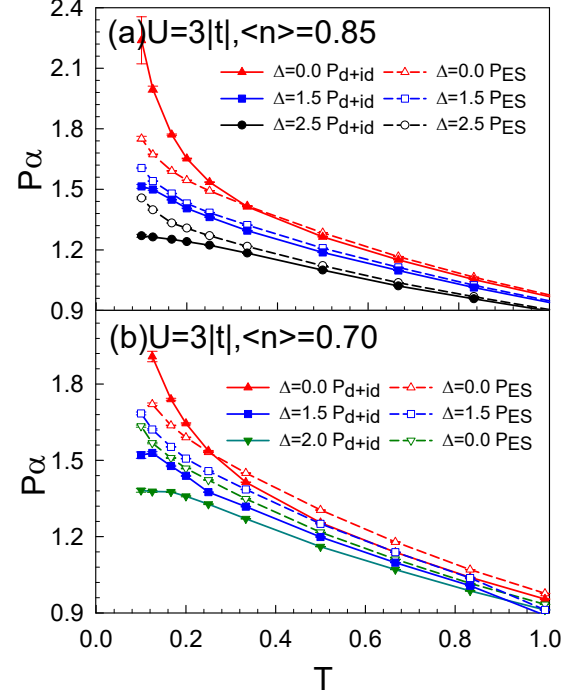


FIG. 5. Pairing susceptibility P_α as a function of temperature T for different pairing symmetries P_{ES} , P_{d+id} , and different disorder strength Δ with electron density (a) $\langle n \rangle = 0.85$ and (b) $\langle n \rangle = 0.70$

disorder, which exhibits a suppressive effect on the $d+id$ wave, leads to the disappearance of $d+id$ effective pairing correlation. In contrast, for the ES wave, disorder has a promoting effect, resulting in the emergence of ES wave that originally lacked ES pairing. Overall, the introduction of disorder shall completely alter the superconducting pairing symmetry at $\langle n \rangle = 0.85$. With increasing disorder strength, the system undergoes three stages: exclusively $d+id$ wave pairing, absence of both $d+id$ and ES wave pairings, and exclusively ES wave pairing.

As doping becomes substantial, the electron density deviates significantly from half-filling at $\langle n \rangle = 0.70$, and the situation undergoes further changes, as shown in Fig. 7. In the clean limit, only $d+id$ effective pairing exists, and the effective pairing correlation for the $d+id$ wave is not particularly large at this point. With the introduction of disorder, it is easily suppressed to become negative, indicating that there is no longer an effective attraction between electrons. Within our computational range, the effective pairing correlation for the ES wave remains consistently negative, indicating that the disorder may not be sufficient to induce ES pairing symmetry at this time.

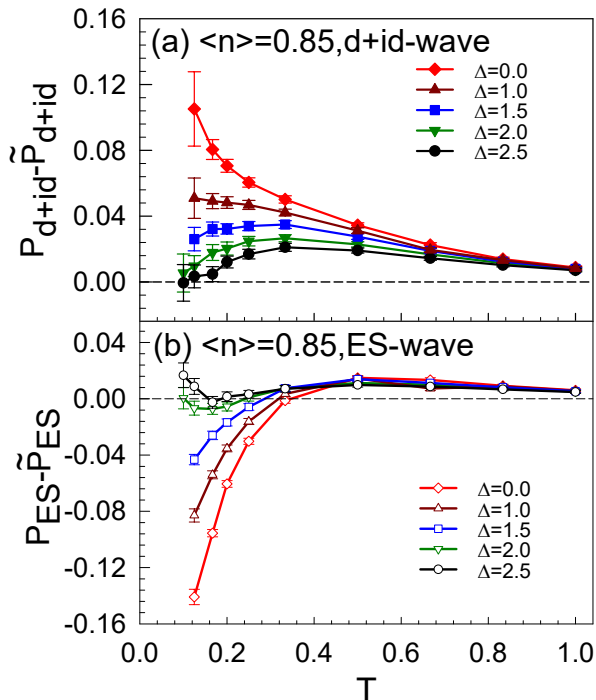


FIG. 6. The effective pairing interaction $P_\alpha - \tilde{P}_\alpha$ in different pairing channels (a) $d+id$ wave and (b) ES wave as a function of temperature T for different disorder strength with electron density $\langle n \rangle = 0.85$.

IV. CONCLUSION

In summary, we utilized the DQMC method to investigate the response of the superconducting order parameter to bond disorder in doped graphene. We focused on computing the pairing susceptibility P_α and effective pairing interaction $P_\alpha - \tilde{P}_\alpha$ for three different electron densities: $\langle n \rangle = 0.95$, $\langle n \rangle = 0.85$, and $\langle n \rangle = 0.70$. We observed that when the electron density was near half-filling ($\langle n \rangle = 0.95$), both the $d+id$ wave and ES wave effective pairing correlations were positive, indicating the coexistence of both pairing waves. In addition, as the disorder strength increases, the system gradually transforms from $d+id$ wave dominance to ES wave dominance, suggesting that a certain strength of disorder can alter the dominant superconducting pairing. Similar behavior was observed at lower electron densities, with the distinction that for lower electron densities, both the $d+id$ and ES wave effective pairing correlations were negative, indicating the absence of these two pairing symmetries. Our calculations may provide insights into the understanding of superconductivity in systems where doping and disorder coexist, as encountered in experiments.

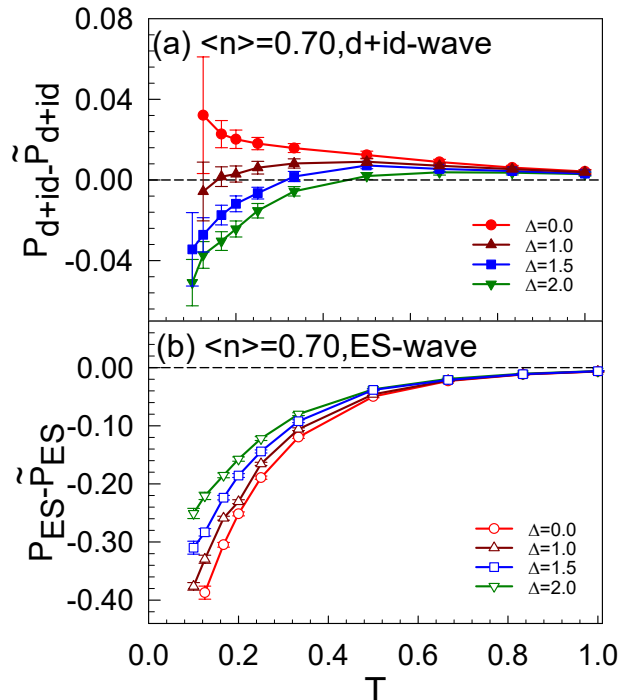


FIG. 7. The effective pairing interaction $P_\alpha - \tilde{P}_\alpha$ in different pairing channels, (a) $d+id$ wave and (b) ES wave, as a function of temperature T for different disorder strength with electron density $\langle n \rangle = 0.70$.

V. ACKNOWLEDGEMENTS

This work was supported by Beijing Natural Science Foundation (No. 1242022) and Guangxi Key Laboratory of Precision Navigation Technology and Application, Guilin University of Electronic Technology (No. DH202322). The numerical simulations in this work were performed at the HSCC of Beijing Normal University.

Appendix A: Convergence of the mean values of measurements

The introduction of bond disorder into the system brings a certain deviation to the results due to the randomness of disorder. To ensure the accuracy of the results, it is necessary to take the average of multiple groups of disordered results. In Fig. 8(a), we show the effective pairing interaction $P_\alpha - \tilde{P}_\alpha$ with the number of disorder realizations. For any given density $\langle n \rangle$, the data does not exhibit significant changes after the number of realizations exceeds ten. We also show the variation as a function of the number of disordered realizations in Fig. 8(b), and the variance curve shows good convergence. In the inset of Fig.8(b), we calculate the average of several sets of data with the number of realizations N set to

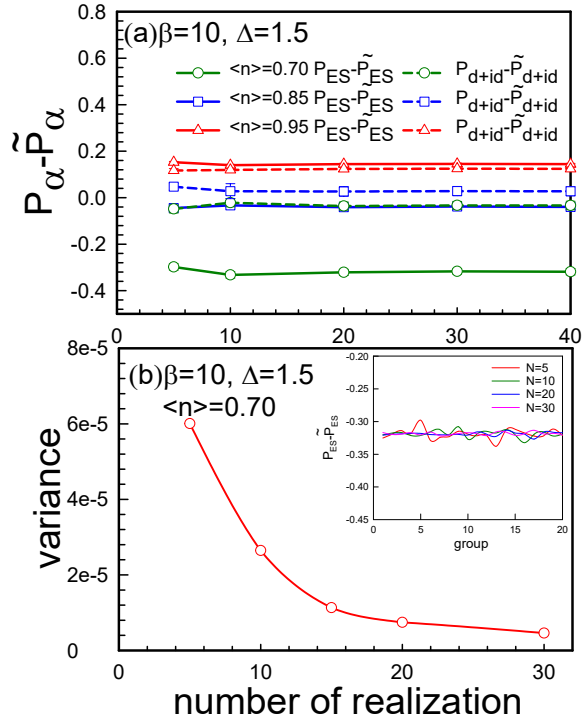


FIG. 8. (a) Effective pairing interaction as a function of number of realization at $\beta = 10$, $\Delta = 1.5$. (b) The corresponding variance of the data in the inset. Inset: The mean value of $P_{ES} - \tilde{P}_{ES}$ as a function of the number of groups. N represents the number of disorder realizations in a group.

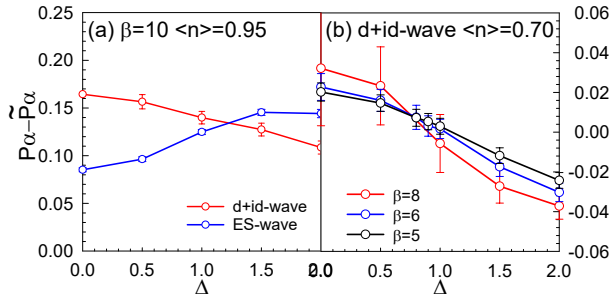


FIG. 9. $P_\alpha - \tilde{P}_\alpha$ as a function of the disorder strength Δ at (a) $\beta = 10$, $\langle n \rangle = 0.95$ for different pairing symmetries and (b) $d + id$ wave at $\langle n \rangle = 0.70$ for different temperatures.

5, 10, 20, and 30, respectively. The results show that the fluctuations are more severe when $N=5$, and are significantly suppressed as N is further increased. This confirms the rationality of using 20 realizations in our main text.

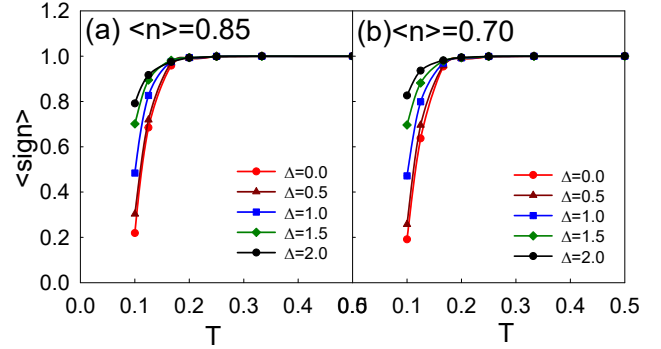


FIG. 10. $\langle \text{sign} \rangle$ as a function of the temperature for different value of bond disorder in (a) $\langle n \rangle = 0.85$ and (b) $\langle n \rangle = 0.70$.

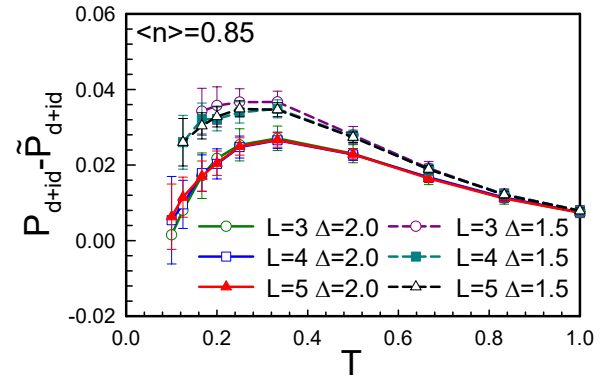


FIG. 11. $P_{d+id} - \tilde{P}_{d+id}$ as a function of the temperature at $\Delta = 1.5$ and $\Delta = 2.0$ for $L = 3, 4, 5$.

Appendix B: The critical point in Fig.1

To determine the critical disorder strength for the transform between dominant SC pairings in Fig. 1, we plot the effective pairing interactions $P_\alpha - \tilde{P}_\alpha$ as functions of Δ , as shown in Fig. 9. In Fig. 9(a), we identify the evolution of $P_{ES} - \tilde{P}_{ES}$ and $P_{d+id} - \tilde{P}_{d+id}$ with disorder for $\langle n \rangle = 0.95$ and $\beta = 10$, which allow us to determine the critical point for the transform of dominant SC pairings. In Fig. 9(b), we plot $P_{d+id} - \tilde{P}_{d+id}$ as a function of Δ at different temperatures for $\langle n \rangle = 0.70$. We find that for $\Delta < \Delta_c$, $P_{d+id} - \tilde{P}_{d+id}$ increases as the temperature is lowered, but for $\Delta > \Delta_c$, $P_{d+id} - \tilde{P}_{d+id}$ decreases with decreasing temperature, indicating that $P_{d+id} - \tilde{P}_{d+id}$ may become negative and is completely suppressed at low temperatures.

Appendix C: Sign problem

Away from half-filling usually leads to sign problems. Related researches have shown that the presence of bond disorder may alleviate the sign problem [55], which is

beneficial for our calculations. In Fig.10, we plot the average fermion sign $\langle sign \rangle$, which is the ratio of the integral of the product of up and down spin determinants to the integral of the absolute value of the product [56]

$$\langle S \rangle = \frac{\sum_{\mathcal{X}} \det M_{\uparrow}(\mathcal{X}) \det M_{\downarrow}(\mathcal{X})}{\sum_{\mathcal{X}} |\det M_{\uparrow}(\mathcal{X}) \det M_{\downarrow}(\mathcal{X})|} \quad (\text{A1})$$

as a function of temperature. When $\langle n \rangle = 0.95$, the system is near half-filling, and the impact of the sign problem is weak, so we mainly show the average sign for (a) $\langle n \rangle = 0.85$ and (b) $\langle n \rangle = 0.70$. As is seen, the sign problem is particularly serious at low temperatures. Fortunately, disorder shall limit and weaken the impact of the sign problem. In order to obtain the same quality of data as $\langle sign \rangle \approx 1$, much longer runs are necessary to compensate the fluctuations. Indeed, we can estimate that the runs need to be stretched [57–59] by a factor on

the order of $\langle sign \rangle^{-2}$. In our simulations, especially in the simulation results where the sign problem is much worse, we have increased measurement from 10000 to 100000 times to compensate the fluctuations, and thus, the results for current parameters are reliable.

Appendix D: Finite-size effect

To make our diagram more convincing, we also checked results on different lattice size. In Fig.11, we take $\langle n \rangle = 0.85$, $\Delta = 1.5$, and $\Delta = 2.0$ as examples, and plot $P_{d+id} - \tilde{P}_{d+id}$ as a function of temperature for different lattice sizes $L = 3$, $L = 4$, and $L = 5$. It can be seen that the finite size has little effect on the results, and there is no qualitative difference in the results at low temperatures, indicating that the $L = 4$ we have chosen can accurately reflect the dominant pairing.

-
- [1] M. Sgrist and K. Ueda, Phenomenological theory of unconventional superconductivity, *Rev. Mod. Phys.* **63**, 239 (1991).
- [2] F. Steglich, J. Aarts, C. D. Bredl, W. Lieke, D. Meschede, W. Franz, and H. Schäfer, Superconductivity in the presence of strong pauli paramagnetism: CeCu_2Si_2 , *Phys. Rev. Lett.* **43**, 1892 (1979).
- [3] T. D. Stanescu and S. Das Sarma, Proximity-induced superconductivity generated by thin films: Effects of fermi surface mismatch and disorder in the superconductor, *Phys. Rev. B* **106**, 085429 (2022).
- [4] M. Leroux, V. Mishra, J. P. C. Ruff, H. Claus, M. P. Smylie, C. Opagiste, P. Rodière, A. Kayani, G. D. Gu, J. M. Tranquada, W.-K. Kwok, Z. Islam, and U. Welp, Disorder raises the critical temperature of a cuprate superconductor, *Proceedings of the National Academy of Sciences* **116**, 10691 (2019).
- [5] A. Słebarski, M. Fijałkowski, M. M. Maška, J. Deniszczyk, P. Zajdel, B. Trump, and A. Yakovenko, Enhancing superconductivity of $\text{Lu}_5\text{Rh}_6\text{Sn}_{18}$ by atomic disorder, *Phys. Rev. B* **103**, 155133 (2021).
- [6] M. A. Tanatar, D. Torsello, K. R. Joshi, S. Ghimire, C. J. Kopas, J. Marshall, J. Y. Mutus, G. Ghigo, M. Zarea, J. A. Sauls, and R. Prozorov, Anisotropic superconductivity of niobium based on its response to nonmagnetic disorder, *Phys. Rev. B* **106**, 224511 (2022).
- [7] H. Hobou, S. Ishida, K. Fujita, M. Ishikado, K. M. Kojima, H. Eisaki, and S. Uchida, Enhancement of the superconducting critical temperature in $\text{Bi}_2\text{Sr}_2\text{CaCu}_2\text{O}_{8+\delta}$ by controlling disorder outside CuO_2 planes, *Phys. Rev. B* **79**, 064507 (2009).
- [8] D. Chakraborty, T. Löfwänder, M. Fogelström, and A. M. Black-Schaffer, Disorder-robust phase crystal in high-temperature superconductors stabilized by strong correlations, *npj Quantum Materials* **7**, 44 (2022).
- [9] E. Arrigoni and S. A. Kivelson, Optimal inhomogeneity for superconductivity, *Phys. Rev. B* **68**, 180503(R) (2003).
- [10] C.-J. Lee and M. Mulligan, Universal conductivity at a two-dimensional superconductor-insulator transition: The effects of quenched disorder and coulomb interaction, *Phys. Rev. B* **108**, 235142 (2023).
- [11] Y. Dubi, Y. Meir, and Y. Avishai, Nature of the superconductor–insulator transition in disordered superconductors, *Nature* **449**, 876 (2007).
- [12] F. Wang, J. Biscaras, A. Erb, and A. Shukla, Superconductor-insulator transition in space charge doped one unit cell $\text{Bi}_2\text{Sr}_1.9\text{CaCu}_2\text{O}_{8+x}$, *Nature Communications* **12**, 2926 (2021).
- [13] Y. Cao, L. Guo, M. Dan, D. E. Doronkin, C. Han, Z. Rao, Y. Liu, J. Meng, Z. Huang, K. Zheng, P. Chen, F. Dong, and Y. Zhou, Modulating electron density of vacancy site by single Au atom for effective CO_2 photoreduction, *Nature Communications* **12**, 1675 (2021).
- [14] V. D. Neverov, A. E. Lukyanov, A. V. Krasavin, A. Vagov, and M. D. Croitoru, Correlated disorder as a way towards robust superconductivity, *Communications Physics* **5**, 177 (2022).
- [15] S.-C. Zhao, L. Gao, Q. Cheng, and Q.-F. Sun, Perfect crossed andreev reflection in the proximitized graphene/superconductor/proximitized graphene junctions, *Phys. Rev. B* **108**, 134511 (2023).
- [16] T. Kamppinen, J. Rysti, M.-M. Volard, G. E. Volovik, and V. B. Eltsov, Topological nodal line in superfluid ^3He and the anderson theorem, *Nature Communications* **14**, 4276 (2023).
- [17] D. Areán, A. Farahi, L. A. Pando Zayas, and A. Salazar Landea, I. and Scardicchio, Holographic p-wave superconductor with disorder, *Journal of High Energy Physics* **2015**, 46 (2015).
- [18] Y. Tanaka, M. Sato, and N. Nagaosa, Symmetry and topology in superconductors –odd-frequency pairing and edge states–, *Journal of the Physical Society of Japan* **81**, 011013 (2012).
- [19] S. C. Holbæk, M. H. Christensen, A. Kreisel, and B. M. Andersen, Unconventional superconductivity protected from disorder on the kagome lattice, *Phys. Rev. B* **108**, 144508 (2023).
- [20] S. Benhabib, C. Lupien, I. Paul, L. Berges, M. Dion, M. Nardone, A. Zitouni, Z. Q. Mao, Y. Maeno,

- A. Georges, L. Taillefer, and C. Proust, Ultrasound evidence for a two-component superconducting order parameter in Sr_2RuO_4 , *Nature Physics* **17**, 194 (2021).
- [21] B. Cheng, D. Cheng, K. Lee, L. Luo, Z. Chen, Y. Lee, B. Y. Wang, M. Mootz, I. E. Perakis, Z.-X. Shen, H. Y. Hwang, and J. Wang, Evidence for d-wave superconductivity of infinite-layer nickelates from low-energy electrodynamics, *Nature Materials* [10.1038/s41563-023-01766-z](https://doi.org/10.1038/s41563-023-01766-z) (2024).
- [22] M. Rigol, B. S. Shastry, and S. Haas, Effects of strong correlations and disorder in d -wave superconductors, *Phys. Rev. B* **79**, 052502 (2009).
- [23] C. C. Tsuei and J. R. Kirtley, Pairing symmetry in cuprate superconductors, *Rev. Mod. Phys.* **72**, 969 (2000).
- [24] J. G. Bednorz and K. A. Müller, Possible high- T_c superconductivity in the Ba-La-Cu-O system, *Zeitschrift für Physik B Condensed Matter* **64**, 189 (1986).
- [25] C. C. Tsuei, J. R. Kirtley, C. C. Chi, L. S. Yu-Jahnes, A. Gupta, T. Shaw, J. Z. Sun, and M. B. Ketchen, Pairing symmetry and flux quantization in a tricrystal superconducting ring of $\text{Yb}_2\text{Cu}_3\text{O}_{7-\delta}$, *Phys. Rev. Lett.* **73**, 593 (1994).
- [26] I. I. Mazin, D. J. Singh, M. D. Johannes, and M. H. Du, Unconventional superconductivity with a sign reversal in the order parameter of $\text{LaFeAsO}_{1-x}\text{F}_x$, *Phys. Rev. Lett.* **101**, 057003 (2008).
- [27] A. V. Chubukov, D. V. Efremov, and I. Eremin, Magnetism, superconductivity, and pairing symmetry in iron-based superconductors, *Phys. Rev. B* **78**, 134512 (2008).
- [28] L.-H. Hu and C. Wu, Two-band model for magnetism and superconductivity in nickelates, *Phys. Rev. Res.* **1**, 032046(R) (2019).
- [29] C. Chen, R. Ma, X. Sui, Y. Liang, B. Huang, and T. Ma, Antiferromagnetic fluctuations and dominant d_{xy} -wave pairing symmetry in nickelate-based superconductors, *Phys. Rev. B* **106**, 195112 (2022).
- [30] Z. Wang, G.-M. Zhang, Y.-f. Yang, and F.-C. Zhang, Distinct pairing symmetries of superconductivity in infinite-layer nickelates, *Phys. Rev. B* **102**, 220501(R) (2020).
- [31] E. Pangburn, L. Haurie, A. Crépieux, O. A. Awoga, A. M. Black-Schaffer, C. Pépin, and C. Bena, Superconductivity in monolayer and few-layer graphene. i. review of possible pairing symmetries and basic electronic properties, *Phys. Rev. B* **108**, 134514 (2023).
- [32] A. Di Bernardo, O. Millo, M. Barbone, H. Alpern, Y. Kalcheim, U. Sassi, A. K. Ott, D. De Fazio, D. Yoon, M. Amado, A. C. Ferrari, J. Linder, and J. W. A. Robinson, p -wave triggered superconductivity in single-layer graphene on an electron-doped oxide superconductor, *Nature Communications* **8**, 14024 (2017).
- [33] D. Perconte, F. A. Cuellar, C. Moreau-Lucaire, M. Piquemal-Banci, R. Galceran, P. R. Kidambi, M.-B. Martin, S. Hofmann, R. Bernard, B. Dlubak, P. Seneor, and J. E. Villegas, Tunable Klein-like tunnelling of high-temperature superconducting pairs into graphene, *Nature Physics* **14**, 25 (2018).
- [34] Y. Cao, V. Fatemi, A. Demir, S. Fang, S. L. Tomarken, J. Y. Luo, J. D. Sanchez-Yamagishi, K. Watanabe, T. Taniguchi, E. Kaxiras, R. C. Ashoori, and P. Jarillo-Herrero, Correlated insulator behaviour at half-filling in magic-angle graphene superlattices, *Nature* **556**, 80 (2018).
- [35] Y. Cao, V. Fatemi, S. Fang, K. Watanabe, T. Taniguchi, E. Kaxiras, and P. Jarillo-Herrero, Unconventional superconductivity in magic-angle graphene superlattices, *Nature* **556**, 43 (2018).
- [36] W. Chen, Y. Chu, T. Huang, and T. Ma, Metal-insulator transition and dominant $d + id$ pairing symmetry in twisted bilayer graphene, *Phys. Rev. B* **101**, 155413 (2020).
- [37] D. M. Kennes, J. Lischner, and C. Karrasch, Strong correlations and $d + id$ superconductivity in twisted bilayer graphene, *Phys. Rev. B* **98**, 241407(R) (2018).
- [38] T. Huang, L. Zhang, and T. Ma, Antiferromagnetically ordered Mott insulator and $d+id$ superconductivity in twisted bilayer graphene: a quantum Monte Carlo study, *Science Bulletin* **64**, 310 (2019).
- [39] B. Roy and V. Juričić, Unconventional superconductivity in nearly flat bands in twisted bilayer graphene, *Phys. Rev. B* **99**, 121407(R) (2019).
- [40] L. Rademaker and P. Mellado, Charge-transfer insulation in twisted bilayer graphene, *Phys. Rev. B* **98**, 235158 (2018).
- [41] A. Crépieux, E. Pangburn, L. Haurie, O. A. Awoga, A. M. Black-Schaffer, N. Sedlmayr, C. Pépin, and C. Bena, Superconductivity in monolayer and few-layer graphene. ii. topological edge states and Chern numbers, *Phys. Rev. B* **108**, 134515 (2023).
- [42] I.-D. Potirniche, J. Maciejko, R. Nandkishore, and S. L. Sondhi, Superconductivity of disordered Dirac fermions in graphene, *Phys. Rev. B* **90**, 094516 (2014).
- [43] H. Dai, J. Hou, X. Zhang, Y. Liang, and T. Ma, Mott insulating state and $d + id$ superconductivity in an ABC graphene trilayer, *Phys. Rev. B* **104**, 035104 (2021).
- [44] E. Lake, A. S. Patri, and T. Senthil, Pairing symmetry of twisted bilayer graphene: A phenomenological synthesis, *Phys. Rev. B* **106**, 104506 (2022).
- [45] S. Pathak, V. B. Shenoy, and G. Baskaran, Possible high-temperature superconducting state with a $d + id$ pairing symmetry in doped graphene, *Phys. Rev. B* **81**, 085431 (2010).
- [46] J. Linder, A. M. Black-Schaffer, T. Yokoyama, S. Doniach, and A. Sudbø, Josephson current in graphene: Role of unconventional pairing symmetries, *Phys. Rev. B* **80**, 094522 (2009).
- [47] T. Ma, Z. Huang, F. Hu, and H.-Q. Lin, Pairing in graphene: A quantum Monte Carlo study, *Phys. Rev. B* **84**, 121410(R) (2011).
- [48] H.-Y. Lu, L. Hao, R. Wang, and C. S. Ting, Ferromagnetism and superconductivity with possible $p + ip$ pairing symmetry in partially hydrogenated graphene, *Phys. Rev. B* **93**, 241410(R) (2016).
- [49] Y.-Z. Chou, F. Wu, J. D. Sau, and S. Das Sarma, Correlation-induced triplet pairing superconductivity in graphene-based moiré systems, *Phys. Rev. Lett.* **127**, 217001 (2021).
- [50] A. Bostwick, J. L. McChesney, K. V. Emtsev, T. Seyller, K. Horn, S. D. Kevan, and E. Rotenberg, Quasiparticle transformation during a metal-insulator transition in graphene, *Phys. Rev. Lett.* **103**, 056404 (2009).
- [51] M. S. Osofsky, S. C. Hernández, A. Nath, V. D. Wheeler, S. G. Walton, C. M. Krowne, and D. K. Gaskill, Functionalized graphene as a model system for the two-dimensional metal-insulator transition, *Scientific Reports*

- 6**, 19939 (2016).
- [52] A. H. Castro Neto, F. Guinea, N. M. R. Peres, K. S. Novoselov, and A. K. Geim, The electronic properties of graphene, *Rev. Mod. Phys.* **81**, 109 (2009).
- [53] T. Ma, L. Zhang, C.-C. Chang, H.-H. Hung, and R. T. Scalettar, Localization of interacting dirac fermions, *Phys. Rev. Lett.* **120**, 116601 (2018).
- [54] L. Tian, Y. Li, Y. Liang, and T. Ma, Doping-dependent metal-insulator transition in a disordered hubbard model, *Phys. Rev. B* **105**, 045132 (2022).
- [55] T. Paiva, E. Khatami, S. Yang, V. Rousseau, M. Jarrell, J. Moreno, R. G. Hulet, and R. T. Scalettar, Cooling atomic gases with disorder, *Phys. Rev. Lett.* **115**, 240402 (2015).
- [56] V. I. Iglovikov, E. Khatami, and R. T. Scalettar, Geometry dependence of the sign problem in quantum monte carlo simulations, *Phys. Rev. B* **92**, 045110 (2015).
- [57] R. R. d. Santos, Introduction to quantum monte carlo simulations for fermionic systems, *Brazilian Journal of Physics* **33**, 36 (2003).
- [58] R. Blankenbecler, D. J. Scalapino, and R. L. Sugar, Monte carlo calculations of coupled boson-fermion systems. i, *Phys. Rev. D* **24**, 2278 (1981).
- [59] G. Yang, S. Xu, W. Zhang, T. Ma, and C. Wu, Room-temperature magnetism on the zigzag edges of phosphorene nanoribbons, *Phys. Rev. B* **94**, 075106 (2016).